Laminin-332 and α3β1 Integrin–Supported Migration of Bronchial Epithelial Cells Is Modulated by Fibronectin

Kristina Kligys[1]*, Yvonne Wu[1]*, Kevin J. Hamill[1]*, Katherine T. Lewandowski[1], Susan B. Hopkinson[1], G. R. Scott Budinger[1], and Jonathan C. R. Jones[1]

[1]Department of Cell and Molecular Biology and Department of Medicine, Division of Pulmonary and Critical Care Medicine, Northwestern University Feinberg School of Medicine, Chicago, Illinois

The repair of the bronchiolar epithelium damaged by cell-mediated, physical, or chemical insult requires epithelial cell migration over a provisional matrix composed of complexes of extracellular matrix molecules, including fibronectin and laminin. These matrix molecules support migration and enhance cell adhesion. When cells adhere too tightly to their matrix they fail to move; but if they adhere too little, they are unable to develop the traction force necessary for motility. Thus, we investigated the relative contributions of laminin and fibronectin to bronchiolar cell adhesion and migration using the immortalized bronchial lung epithelial cell line (BEP2D) and normal human bronchial epithelial (NHBE) cells, both of which assemble a laminin α3β3γ2 (LM332)/fibronectin-rich matrix. Intriguingly, BEP2D and NHBE cells migrate significantly faster on an LM332-rich matrix than on fibronectin. Moreover, addition of fibronectin to LM332 matrix suppresses motility of both cell types. Finally, fibronectin enhances the adhesion of both BEP2D and NHBE cells to LM332-coated surfaces. These results suggest that fibronectin fine tunes LM332-mediated migration by boosting bronchiolar cell adhesion to substrate. We suggest that, during epithelial wound healing of the injured airway, fibronectin plays an important adhesive role for laminin-driven epithelial cell motility by promoting a stable cellular interaction with the provisional matrix.

Keywords: motility; adhesion; extracellular matrix

The epithelial cell sheet lining the bronchial airway is a selective barrier that allows the passage of solutes and ions, but prevents pathogens or pollutants moving from the epithelial lumen into the connective tissue. Prolonged exposure to cigarette smoke, inhaled irritants, or respiratory allergens damages the epithelial cells lining the bronchial airway and compromises the barrier function of the epithelium. Activation of the immune system can worsen epithelial damage. As a result, many chronic respiratory diseases, including asthma and chronic obstructive pulmonary disease, are characterized by basement membrane thickening, epithelial cell shedding, and a loss of epithelial barrier integrity (1, 2). Repair of the damaged airway epithelium requires the migration of undamaged epithelial cells or epithelial progenitor cells to the sites of airway injury.

Wound healing in the bronchial epithelium is a multistep process involving the detachment of unwounded epithelial cells from their matrix, rearrangement of their cytoskeletons, development of traction forces necessary for directed migration over the wound, establishment of new interactions with the wound surface via the binding of receptors to matrix proteins covering the wound bed, and the orchestration of assembly of a new basement membrane (3, 4). The focus of the current study was to gain new insight into the role that extracellular matrix proteins and matrix receptors play in regulating the migration of bronchial epithelial cells. In this regard, bronchial epithelial cells neighboring the wound area deposit a provisional extracellular matrix rich in fibronectin, but that also contains laminin (primarily, laminin α3β3γ2 [LM332]) over which they move during the healing process (5–7). Moreover, evidence has been presented that α3β1 and α6β4 integrin matrix receptors are required for epithelial cell migration on LM332, whereas α5β1 integrin is required for migration on fibronectin during wound repair (3, 8, 9).

In vitro studies indicate that, individually, a number of components, including fibronectin and laminin, of the provisional matrix of a wound in the bronchial epithelium support epithelial cell migration (10, 11). However, *in vivo*, bronchial epithelial cells migrate over a multiprotein provisional matrix. This raises the possibility that complex mixes of matrix proteins in the provisional matrix might differentially regulate bronchial epithelial cell migration. To test this hypothesis we used an immortalized bronchial cell line (BEP2D) and normal human bronchial epithelial (NHBE) cells, both of which deposit a matrix that mirrors the provisional matrix of the wound bed, at least with regard to fibronectin and laminin deposition. We then analyzed the migration of BEP2D and NHBE cells on matrices assembled by cells, individual matrix components, or matrices containing combinations of extracellular matrix proteins *in vitro*. Our results confirm previous reports that laminin-rich matrices support bronchial cell migration, although only BEP2D cells move efficiently on fibronectin (10, 11). In addition, our data indicate that both immortalized and normal bronchiolar epithelial cells migrate significantly faster on an LM332-rich matrix than on fibronectin. Intriguingly, our results reveal that, in a complex matrix, fibronectin suppresses laminin-supported bronchiolar epithelial cell migration. We also evaluated the role of integrins in regulating laminin-driven migration of BEP2D cell motility, and our studies demonstrate an important role for α3β1 integrin in determining their speed.

MATERIALS AND METHODS

Cell Culture, Antibodies, and Reagents

The immortalized human bronchial epithelial cell line, BEP2D, was a generous gift of Dr. Curtis C. Harris of the National Institutes of

(*Received in original form December 11, 2012 and in final form March 22, 2013*)

* These authors contributed equally to this study.

This work was supported by National Institutes of Health grant RO1 HL092963 (J.C.R.J. and G.R.S.B.). Technical aspects of the work were additionally supported by the Northwestern University Flow Cytometry and Cell Imaging Facilities, Cancer Center Support Grant CA060553.

Author Contributions: J.C.R.J. and G.R.S.B. directed the project. K.K., K.J.H., and J.C.R.J. prepared the manuscript. K.K., K.J.H., Y.W., and K.T.W. conducted experiments and performed data analyses. S.B.H. designed and performed the adhesion assays and generated lentiviral vectors.

Correspondence and requests for reprints should be addressed to Jonathan C. R. Jones, Ph.D., Department of Cell and Molecular Biology, Feinberg School of Medicine, Northwestern University, 303 East Chicago Avenue, Chicago, IL 60611. E-mail. j-jones3@northwestern.edu

This article has an online supplement, which is accessible from this issue's table of contents at www.atsjournals.org

Am J Respir Cell Mol Biol Vol 49, Iss. 5, pp 731–740, Nov 2013

Originally Published in Press as DOI: 10.1165/rcmb.2012-0509OC on April 13, 2013
Internet address: www.atsjournals.org

Health, and was described previously (12). The cells were maintained in LHC-9 media (Life Technologies, Grand Island, NY) supplemented with a 1% penicillin/streptomycin mixture (Sigma-Aldrich, St. Louis, MO) and grown at 37°C. Immortalized human epidermal keratinocytes (iHEKs), immortalized with human papilloma virus genes E6 and E7, were described previously (13). NHBE cells were purchased from Lonza Ltd. (Waterville, MD) and cultured as outlined by the supplier. J1B5, a rat monoclonal antibody against α6 integrin, was a generous gift of Dr. Caroline Damsky (University of California, San Francisco). Mouse monoclonal antibodies against α2 integrin (P1E6), α3 integrin (P1B5), α6 integrin (4F10), β1 integrin (12G10) β4 integrin (3E1), and the γ2 subunit of LM332 (D4B5) were purchased from Millipore (Billerica, MA). A monoclonal rabbit antibody against paxillin was obtained from Epitomics (Burlingame, CA). A rabbit polyclonal antibody against the light chain of α6 integrin was a generous gift of Dr. Anne Cress (University of Arizona). The rabbit polyclonal antibody against fibronectin was purchased from Sigma-Aldrich. The mouse monoclonal antibody against the β3 subunit of LM332 was obtained from BD Transduction Laboratories (San Jose, CA). Fibronectin from human plasma was purchased from Sigma-Aldrich. LM332 conditioned medium was derived from iHEK cells. Fibronectin small interfering (si)RNA (5′-AACAAATCTCCTG CCTGGGAC-3′) was purchased from Qiagen (Chatsworth, CA).

Gel Electrophoresis and SDS-PAGE

Matrix was prepared as detailed elsewhere (14). Briefly, subconfluent cells plated on tissue culture dishes were washed in sterile PBS. The cells were treated with 20 mM NH_4OH for 5 minutes at 37°C. The cells were removed and the remaining matrix was washed several times with distilled water. The resulting matrix was solubilized in a urea/SDS sample buffer. The proteins were separated by SDS-PAGE, transferred to nitrocellulose, and processed for immunoblotting as previously described (15). To quantify the amount of fibronectin deposited by cells, cultures were first imaged and the numbers of cells in a given area determined. The solubilized matrix of a given number of cells in a 1-cm^2 area was processed for immunoblotting.

Fluorescence-Activated Cell Sorting

Cells were trypsinized, resuspended in a 1:1 mix of PBS and normal goat serum, and incubated with mouse monoclonal antibodies against α2, α3, α6, β1, or β4 integrins at room temperature for 45 minutes. The cells were washed with PBS and incubated with FITC-conjugated secondary antibody for 45 minutes at room temperature in the dark. Integrin cell surface expression was analyzed using a Beckman Coulter CyAn flow cytometer (Beckman Coulter, Pasadena, CA). As a negative control, primary antibody was omitted.

Fluorescence Microscopy

Cells were plated onto glass coverslips and processed for microscopic analyses as detailed previously (16). All preparations were viewed with a Zeiss laser scanning 510 confocal microscope (Zeiss Inc., Thornwood, NY). Images were exported as TIFF files, and figures were generated using Adobe Photoshop software (Adobe Systems, San Jose, CA).

Cell Motility

Single cell motility was measured as described previously (15). Briefly, in most of the studies, cells were plated onto matrices that were prepared as previously described (14). After a 2-hour attachment, the motility assay was begun. However, in one distinct set of assays, BEP2D and NHBE cells were plated onto uncoated substrate and, after an overnight incubation, the motility of cells was then monitored. In all instances, cells were viewed on a Nikon TE2000 inverted microscope (Nikon Inc., Melville, NY). Images were taken at 2-minute intervals over 1 hour. Cell motility behavior was tracked using the MetaMorph Imaging System (Universal Imaging Corp., Molecular Devices, Downingtown, PA). Vector diagrams displaying the migration tracks of 10 randomly selected cells relative to their start point were plotted for each assay condition. Migration speed was calculated as the total distance migrated over time. Processivity was calculated as the ratio of maximum distance obtained relative to the origin versus total distance traveled.

In addition to the single-cell motility assays described previously here, the motility of BEP2D cell groups was also evaluated (17). In brief, BEP2D cells were plated in growth medium, supplemented with $CaCl_2$ to a final concentration of 2 mM, within the confines of a plastic 6-mm-diameter ring positioned at the center of a matrix-coated glass coverslip. At 2 hours, the ring was removed. In this "outgrowth" model, cells migrate as a sheet from the confluent area originally delineated by the ring. Cells were imaged by phase-contrast microscopy immediately after removal of the ring and after 6 hours of migration over "fresh" substrate. The distance migrated over this time course was determined by measuring the cell sheet radii at 16 regular spaced intervals around each circle.

Lentiviral Construct

To express small hairpin RNA targeted against α6 integrin expression, the BLOCK-iT Lentiviral RNAi Expression System was used (Invitrogen Corp., Carlsbad, CA). Two complementary single-stranded DNA oligonucleotides (21-mers) derived from the human *ITGA6* gene were synthesized, annealed, and cloned into the pENTR/U6 entry vector (Invitrogen Corp.). A lambda recombination was performed between the entry construct and the pLenti6/BLOCK-iT-DEST vector to generate an expression construct. To produce lentivirus, the expression construct was transfected into the 293FT packaging cell line. The lentiviral stock was titered and BEP2D cells were infected at a multiplicity of infection of 1:10 in cell medium. Cells expressing the α6 integrin small hairpin RNA were selected by resistance to blasticidin and then cloned by limiting cell dilution. Clones were assayed for knockdown by immunoblotting and fluorescence-activated cell sorting.

Statistical Analysis

Statistical significance was determined by ANOVA and two tailed Student's *t* test. A P value of 0.05 or less was considered statistically significant.

RESULTS

Expression of Matrix Proteins and Integrin Receptors by BEP2D and NHBE Cells

BEP2D cells were generated by immortalizing human bronchial epithelial cells with human papillomavirus (12). BEP2D cells are nontumorigenic, grow in an anchorage-dependent manner, and are contact growth inhibited. BEP2D cells and their normal counterparts (NHBE) were prepared for immunofluorescence and matrix preparations processed for immunoblotting using antibodies against the γ2 or β3 subunit of LM332 and fibronectin. Immunofluorescence imaging revealed that both BEP2D and NHBE cells deposit LM332 as they spread and/or move across their substrate. Interestingly, fibrils of fibronectin are found under the cells and outline deposits of LM332 (Figure 1A). Immunoblotting analyses of preparations of matrix proteins derived from cultures of BEP2D and NHBE cells also reveal that they deposit a matrix rich in fibronectin and LM332, using the reactivity of a β3 laminin subunit antibody as an indicator of the presence of LM332 (Figure 1B). Fibronectin and LM332 in the matrix of BEP2D and NHBE cells imply that they both deposit extracellular matrix proteins that mirror, at least in part, that of the provisional matrix elaborated by epithelial cells in the wounded airway (5–7).

Intriguingly, the matrix composition of BEP2D differs from that of iHEKs, which deposit a matrix primarily composed of LM332 with very little, if any, fibronectin (Figure 1C) (18).

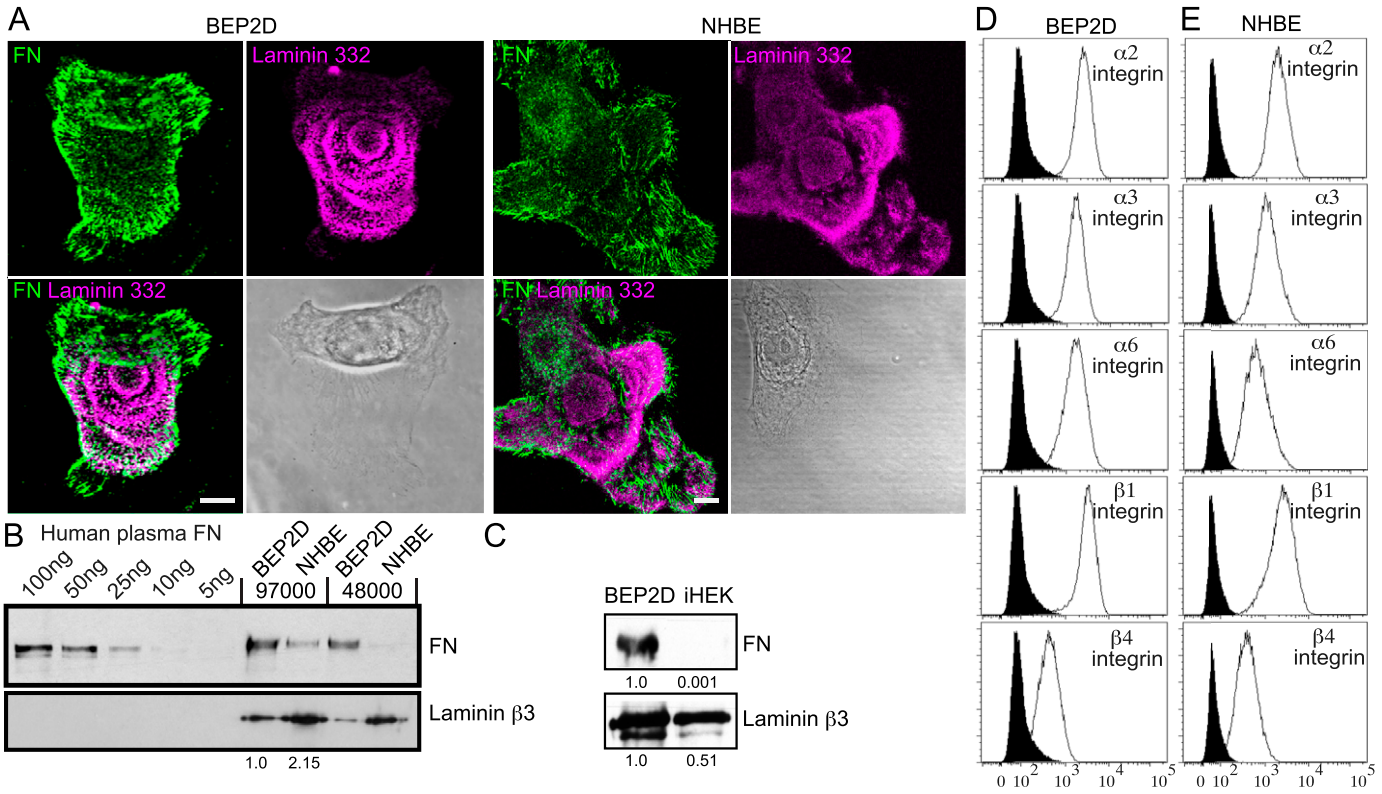

Figure 1. Composition of matrix deposited by bronchial epithelial cell line, BEP2D, and normal human bronchial epithelial (NHBE) cells and their integrin profiles. (*A*) BEP2D and NHBE cells were plated on uncoated glass coverslips overnight. The preparations were then fixed and stained with antibodies against laminin $\alpha 3\beta 3\gamma 2$ (laminin-332 [LM332]; the $\gamma 2$ subunit) and fibronectin (FN), as indicated. The *lower left panel* in each set of four shows the *overlay* of the images. The *lower right panel* in each set of four shows a phase-contrast image of the stained cell. (*B*) The indicated concentrations of human FN and matrix preparations derived from the indicated numbers of BEP2D and NHBE cells from the same surface area at 72 hours after plating were prepared for immunoblotting using an FN and LM332 (the $\beta 3$ subunit). (*C*) Immunoblot analyses of extracellular matrix extracts prepared from equal numbers of immortalized human epidermal keratinocyte (iHEK) and BEP2D cells at 72 hours after plating on untreated tissue culture dishes. Matrix preparations were probed with antibodies against the laminin $\beta 3$ subunit and FN, as indicated. Blots were scanned and the relative values are shown numerically. (*D* and *E*) Surface expression of $\alpha 2$, $\alpha 3$, $\alpha 6$, $\beta 1$, and $\beta 4$ integrins in BEP2D and NHBE cells was measured by fluorescence-activated cell sorting (FACS; *open histograms*). *Filled histograms* represent secondary antibody alone. *Scale bars* in (*A*), 10 μm.

BEP2D cells deposit about twofold the levels of LM332 as iHEK and half the amount deposited by NHBE at 72 hours after plating (Figure 1B). In contrast, NHBE cells deposit approximately fivefold less fibronectin than BEP2D cells. We also quantified the amount of fibronectin in BEP2D and NHBE cell matrix by comparing the immunoblotting reactivity of a fibronectin antibody with known amounts of fibronectin to that of a cell matrix protein preparation, derived from a known quantity of cells in a given area at 72 hours after plating (Figure 1B). Specifically, over a 72-hour period, 5×10^4 BEP2D cells deposit in the range of 70–100 ng fibronectin/cm^2. For all subsequent analyses, we used fibronectin at a coating of approximately 100 ng/cm^2.

Our next goal was to assess the integrin matrix receptor expression profile of BEP2D and NHBE cells. Fluorescence-activated cell sorting analyses indicated that both cell types display $\alpha 2$, $\alpha 3$, $\alpha 6$, $\beta 1$, and $\beta 4$ integrin subunits on their surface (Figure 1D). The integrin profile of NHBE cells is consistent with other reports (19). In addition, the localization pattern of each integrin subunit was determined by immunostaining BEP2D and NHBE cells. In some instances, double labeling was performed using antibodies against both integrins and paxillin, a marker of focal contacts/adhesions (Figures 2 and 3). In both BEP2D and NHBE cells, $\alpha 3$ integrin subunits localized to focal contacts stained by paxillin antibodies. The $\alpha 2$ integrin subunit was found in some focal contacts at the cell edge in both cell types, but was also found at regions of cell–cell interaction in contacting NHBE cells (Figures 2 and 3). $\alpha 6$ integrin displayed a limited codistribution with $\beta 1$ integrin in BEP2D cells, but they exhibited little, if any, colocalization in NHBE cells (Figures 2 and 3). Rather, $\alpha 6$ integrin localized in swirls or rosette-like patterns along the substratum attached surface of both cell types, and was detected in the matrix left behind by NHBE cells in some instances (Figures 2 and 3). Moreover, $\alpha 6$ integrin showed precise colocalization with $\beta 4$ integrin in both BEP2D and NHBE cells (Figures 2 and 3).

Migration of BEP2D and NHBE Cells on Extracellular Matrix Components

Human keratinocytes migrate on LM332-rich matrix (13, 20). In contrast, fibronectin in the matrix of mouse keratinocytes appears to inhibit LM332-mediated skin cell motility (18). The presence of both fibronectin and LM332 in the matrix deposited by BEP2D and NHBE cells led us to compare the motility phenotype of both cell types on various substrates. We first assayed the motility behavior of BEP2D cells on their own matrix, the LM332-rich matrix deposited by iHEKs, LM332 from conditioned medium, and fibronectin. BEP2D cells plated on BEP2D matrix, iHEK matrix, and fibronectin exhibited similar patterns of cell motility (i.e., displayed comparable levels of

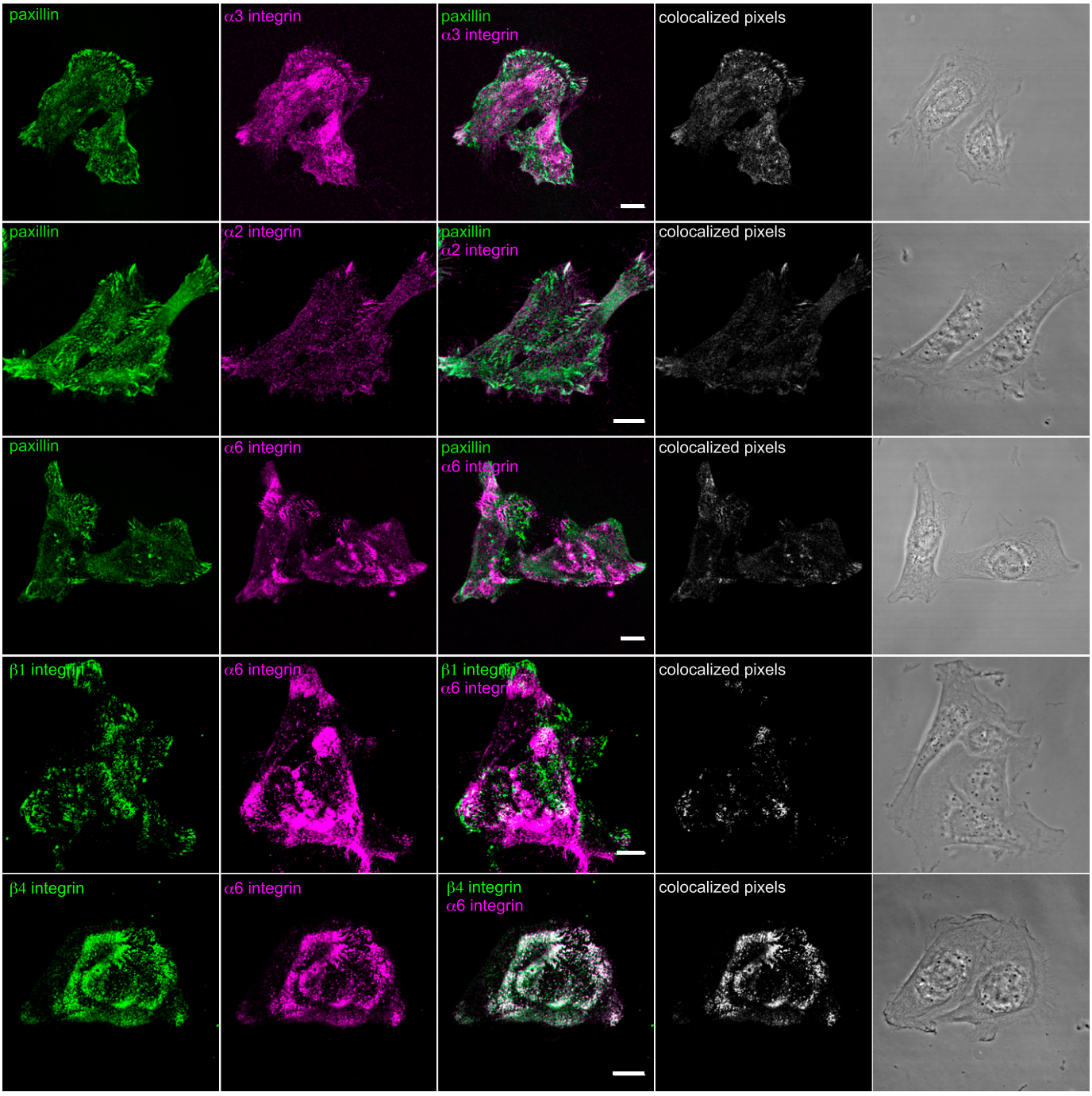

Figure 2. Integrin localization in BEP2D cells. Cells were plated on uncoated glass coverslips overnight, fixed, and stained with antibodies against α2 integrin, α3 integrin, and α6 integrin, in combination with antibodies against paxillin, as indicated. In addition, cells were also prepared for double labeling using either a combination of antibodies against β1 and α6 integrin or β4 and α6 integrin. Overlays of the single stain images are shown in the *third column*. In the *fourth column*, colocalized pixels are presented. The micrographs in the *fifth column* show phase-contrast images of the fixed and stained cells. *Scale bars*, 10 μm.

directed migration [Figures 4A and 4B]). Interestingly, BEP2D cells showed significantly reduced directional persistence when moving on LM332 (Figure 4B). This likely reflects the random nature of the arrangement of the latter in contrast to the "organized" LM332 deposited by cells onto substrate. Nevertheless, the speeds of BEP2D cells on the various matrices are quite distinct. BEP2D cells exhibited faster motility on iHEK matrix and LM332 when compared with when they move on their own matrix (Figure 4C, Table 1). There was no significant difference in cell speed of BEP2D cells moving on fibronectin when compared with when they move on their own matrix (Figure 4C, Table 1).

We next investigated whether the presence of fibronectin alters the speed of BEP2D cells migrating on iHEK matrix and LM332 (Figure 5). To do so, we plated BEP2D cells on iHEK matrix or LM332 supplemented with fibronectin. Although the presence of fibronectin did not affect directional persistence (Figures 5B and 5E), fibronectin reduced the

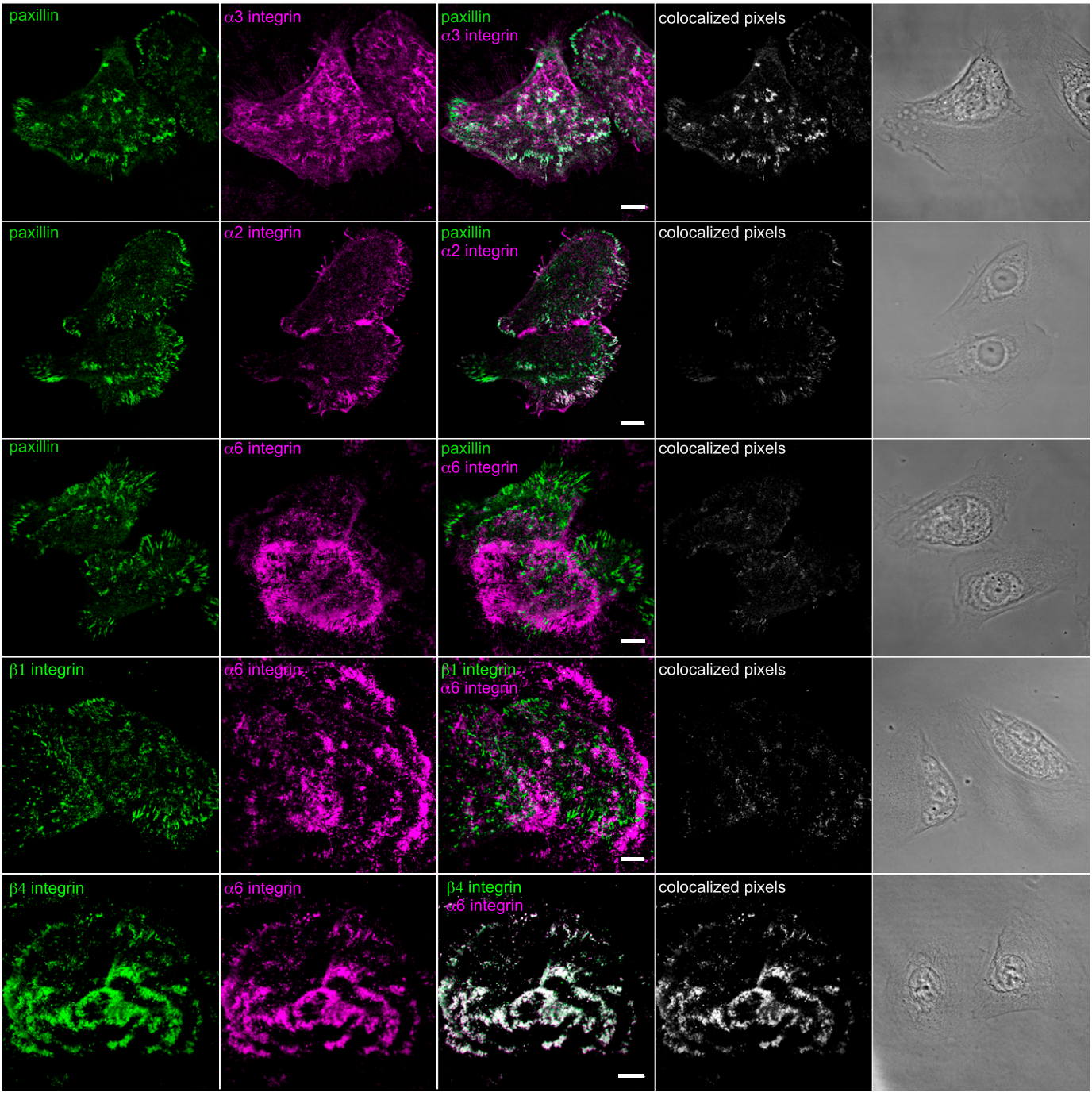

Figure 3. Integrin localization in NHBE cells. Cells were plated on uncoated glass coverslips overnight, fixed, and stained with antibodies against α2 integrin, α3 integrin, and α6 integrin, in combination with antibodies against paxillin, as indicated. In addition, cells were also prepared for double labeling using either a combination of antibodies against β1 and α6 integrin or β4 and α6 integrin. Overlays of the single stain images are shown in the *third column*. In the *fourth column*, colocalized pixels are presented. The micrographs in the *fifth column* show phase-contrast images of the fixed and stained cells. *Scale bars*, 10 μm.

migration speed of BEP2D cells on iHEK matrix and LM332 (Figures 5C and 5F). Moreover, we also evaluated the migration of BEP2D moving from a confluent patch of cells at the center of a coverslip onto a substrate coated with either LM332, fibronectin, or LM332 supplemented with fibronectin (Figure 5H, Table 2). BEP2D cells moved with higher velocity over LM332 than fibronectin. Moreover, fibronectin addition reduced the velocity of the cells in this assay (Figure 5G; *see also* Figure E1E in the online supplement).

To assess whether the above results are peculiar to BEP2D or are reflective of bronchiolar epithelial cell motility in general, we also evaluated NHBE migration on LM332, with and without supplementation with fibronectin, and fibronectin alone. NHBE cells moved with approximately the same persistence as BEP2D cells on LM332, with and without addition of fibronectin (Figures 6A and 6B). However, unlike BEP2D cells, the persistence of NHBE cells was reduced when the cells were plated on fibronectin when compared with their motility on LM332. This likely

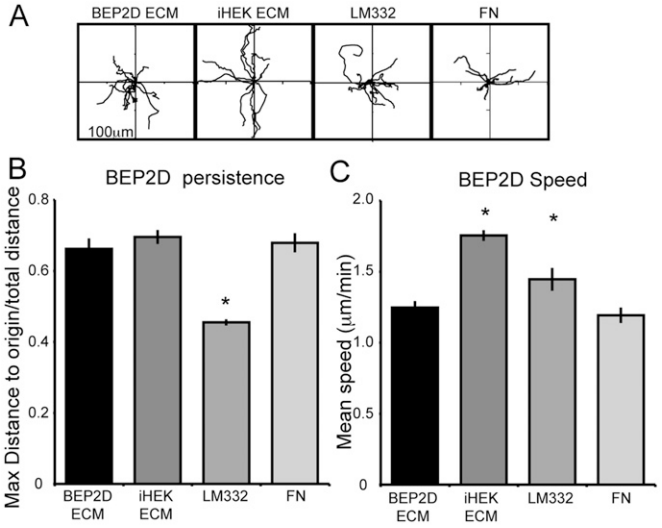

Figure 4. Extracellular matrix components and their influence on the motility BEP2D cells. (*A*) Rose plots depict the individual migration patterns of 10 randomly selected BEP2D cells moving on BEP2D matrix, iHEK matrix, LM332, or FN. In all assays, the cells were allowed to adhere to the matrix for 2 hours and cell migration was tracked for 1 hour. (*B* and *C*) Graphical representation of persistence and speed of the cells (±SEM) as in (*A*). *Significant differences, $P < 0.05$, relative to cells moving on BEP2D matrix, as determined by ANOVA and Student's *t* test. ECM, extracellular matrix.

reflects the overall reduced motility exhibited by the NHBE cells plated onto fibronectin rather than a defect in persistence *per se* (Figure 6B). Furthermore, the speed of NHBE was significantly reduced on LM332 supplemented with fibronectin when compared with their speed moving on LM332 alone (Figure 6C; Table 1).

Because the above data reveal that fibronectin reduces the speed of both BEP2D and NHBE cells moving on LM332-rich matrices, we wondered whether it would impact their adhesion to LM332-coated surfaces. To assess this possibility, we evaluated cell attachment to surfaces coated with LM332 with and without fibronectin supplementation. Fibronectin dramatically enhanced the adhesion of both BEP2D and NHBE cells to LM332 (Figures 5H and 6D).

LM332 Receptor and the Regulation of BEP2D Migration

LM332 matrix supports cell adhesion and migration in an α6β4 and/or α3β1 integrin–dependent manner (13, 20–25). Because our results indicate that LM332 promotes bronchial epithelial cell migration, we next wished to assess which integrin receptor is responsible for regulating such motility. For these and subsequent studies, we focused on BEP2D cells, as we could generate clonal populations exhibiting a knockdown in expression of the LM332 receptor α6β4 integrin (Figure 7A). Consistent with our recent findings in human keratinocytes (20), knockdown of α6 integrin expression in BEP2D cells led to a decrease in β4 integrin surface expression (Figure 7B). However, in contrast to our previous findings in keratinocytes, loss of α6β4 integrin expression in BEP2D cells did not affect surface expression of α3 integrin (Figure 7B). In keratinocytes, we demonstrated that α3 integrin expression is regulated by α6β4 integrin via 4EBP1, a translational repressor protein that binds and inhibits the activity of translation initiation factor 4E (20, 26, 27). However, in α6 integrin knockdown BEP2D cells, the phosphorylation of 4EBP1 was maintained or even increased (Figure 7C). Thus, α6β4 integrin–independent activation of 4EBP1 in α6 integrin knockdown BEP2D cells explains why their α3 integrin subunit expression was unaffected. This difference allowed us to evaluate the distinct roles of α6β4 integrin and α3β1 integrin in mediating LM332 matrix–supported migration without the complication of the type of integrin crosstalk we have observed in skin cells. Thus, we tracked the migration of α6 integrin knockdown BEP2D cells plated on wild-type BEP2D matrix (Figure 7D). In contrast to our results in keratinocytes, loss of α6β4 integrin expression in the bronchial epithelial cells did not affect persistence when the cells moved on BEP2D matrix (Figure 7E). In addition, wild-type and α6 integrin knockdown BEP2D cells migrated with a similar speed (Figure 7F, Table 1). This suggests that α3 rather than α6 integrin determines cell speed in BEP2D cells moving on their own matrix. To confirm this, we assayed the motility of the α6 integrin knockdown BEP2D cells on wild-type BEP2D matrix in the presence of an α3 integrin antagonist (Figures 7D and 7F). The speed of the treated cells was significantly reduced compared with α6 integrin knockdown cells in the absence of an α3-inhibiting antibody, as well as when compared with wild-type BEP2D cells moving on BEP2D matrix (Figure 7F, Table 1). Moreover, as a negative control, α6 integrin knockdown BEP2D cells were plated on wild-type matrix in the presence of an α2 integrin antagonist. Inhibiting α2 integrin function in the α6 integrin knockdown BEP2D cells did not alter their speed of migration (Figure 7F, Table 1).

Published data from our group indicate that α6 integrin regulates directed migration of skin cells by determining the deposition of LM332 onto the substrate (13). In sharp contrast, α6 integrin knockdown BEP2D cells show similar directed migration to their wild-type counterparts. This led us to assess whether the deposition of fibronectin might compensate in the α6 integrin knockdown BEP2D cells, and allow them to migrate directionally. To test this possibility, we induced a decrease in expression of fibronectin in α6 integrin knockdown BEP2D cells using siRNA (Figure 7G). We confirmed fibronectin knockdown by immunoblotting (Figure

TABLE 1. SPEED OF BRONCHIAL EPITHELIAL CELL LINE BEP2D AND NORMAL HUMAN BRONCHIAL EPITHELIAL CELLS MOVING ON THE INDICATED SUBSTRATES UNDER THE SPECIFIED CONDITIONS

Line/Treatment	Matrix	Speed (μm/min)
BEP2D	BEP2D ECM	1.25 ± 0.04
	iHEK ECM	1.75 ± 0.04
	LM332	1.45 ± 0.09
	FN	1.19 ± 0.05
	iHEK ECM+FN	1.59 ± 0.01
	LM332 + FN	1.12 ± 0.02
BEP2D α6 shRNA	BEP2D ECM	1.21 ± 0.05
BEP2D α6 shRNA + P1B5	BEP2D ECM	0.97 ± 0.08
BEP2D α6 shRNA + P1E6	BEP2D ECM	1.27 ± 0.05
BEP2D	No precoat*	1.53 ± 0.04
BEP2D α6 shRNA	No precoat*	1.57 ± 0.08
BEP2D α6 shRNA FNsiRNA	No precoat*	1.39 ± 0.04
NHBE	No precoat*	1.56 ± 0.02
NHBE	LM332	1.77 ± 0.14
	FN	0.82 ± 0.04
	LM332+FN	1.37 ± 0.09

Definition of abbreviations: BEP2D, bronchial epithelial cell line BEP2D; ECM, extracellular matrix; FN, fibronectin; iHEK, immortalized human epidermal keratinocyte; LM332, laminin α3β3γ2; NHBE, normal human bronchial epithelial; shRNA, small hairpin RNA; siRNA, small interfering RNA.

*In these assays the speed of the cells was determined following overnight plating onto an uncoated substrate.

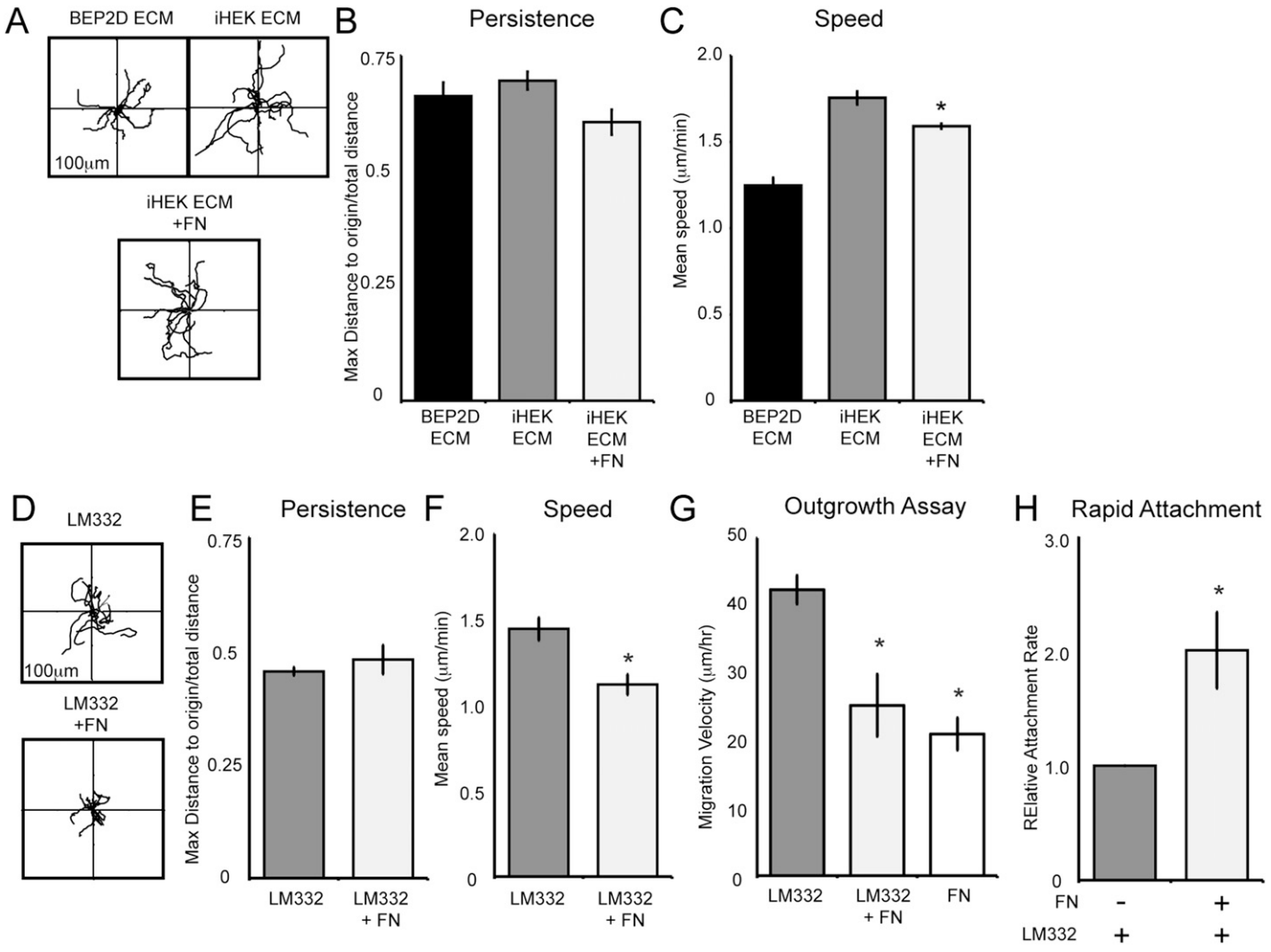

Figure 5. BEP2D cell migration speed is regulated by FN in the matrix. (*A*) Vector diagrams depicting the individual migration patterns of 10 randomly selected BEP2D cells plated on BEP2D matrix, iHEK matrix, or iHEK matrix to which FN was added. The cells were allowed to adhere to the matrix for 2 hours and the migration of the cells was tracked for 1 hour. (*B* and *C*) Graphical representation of the persistence and speed of BEP2D cells as in (*A*). (*D*) BEP2D motility on LM332 or LM332 to which FN was added. (*E* and *F*) Graphical representation of the persistence and speed of cells as in (*D*). (*G*) Velocity of BEP2D cells moving outwards from a confluent monolayer onto LM332, LM332 supplemented with FN (LM332 + FN), or FN alone. (*H*) Depicts a rapid attachment assay evaluating the adhesion of BEP2D cells to LM332 or LM332 supplemented with FN (±FN) at 1 hour after plating. The individual *bars* of the graph represent means (±SEM) relative to attachment to LM332. All assays were performed in triplicate. For motility assays, roughly 60 cells were tracked per assay. *Significant differences, relative to cells migrating on iHEK matrix or LM332, as determined by ANOVA and Student's *t* test.

7G). Moreover, the fibronectin siRNA had little effect on expression of the β3 subunit of LM332 (Figure 7G). We then evaluated motile behavior of the fibronectin knockdown cells (Figures 7G and 7H). In this experiment, the motility of cells was evaluated after overnight plating on uncoated surfaces. In other words, we assayed migration of the cells without replating onto matrix, but rather upon the matrix they themselves deposited over 20–24 hours after plating. The dual knockdown cells exhibited aberrant motility and a reduced ability to migrate in a persistent fashion, although there was no effect on their speed (Figures 7H–7J). Taken together with the results presented in Figure 5, these studies indicate that, when fibronectin expression is inhibited, α6β4 integrin regulates directed migration of BEP2D cells, whereas α3β1 integrin determines their speed. These results are consistent with our studies on keratinocytes (13, 19).

DISCUSSION

In this study, we compared the organization and composition of matrix deposited by an immortalized bronchial epithelial cell line (BEP2D) with that of primary passaged bronchial epithelial (NHBE) cells. Our results indicate that both deposit a matrix rich in LM332 and fibronectin, although there are differences in the absolute amounts and relative ratios of fibronectin to laminin in the matrix of these related, but distinct, cell types. Moreover, BEP2D and NHBE cells express closely equivalent levels of integrin subunits, which show similar distributions at the cell surface. Based on the latter result, we suggest that BEP2D cells are good substitutes for primary bronchiolar cells when looking at the effects of matrix on integrin-mediated signaling events leading to specific motility behavior.

It has long been established that components of the extracellular matrix play important roles in regulating epithelial cell adhesion to and migration over a wound bed. In this study, our data

TABLE 2. MIGRATION VELOCITIES OF BRONCHIAL EPITHELIAL CELL LINE BEP2D CELLS MOVING AS A SHEET UPON THE INDICATED SUBSTRATES

Line	Matrix	Velocity ($\mu m/min$)
BEP2D-outgrowth	LM332	1.25 ± 0.04
	FN	1.75 ± 0.04
	LM332 + FN	1.45 ± 0.09

Definition of abbreviations: BEP2D, bronchial epithelial cell line BEP2D; FN, fibronectin; LM332, laminin $\alpha3\beta3\gamma2$.

indicate that fibronectin and LM332 each sustain the directed migration of BEP2D cells, with fibronectin supporting more persistent motility of BEP2D cells than LM332. In contrast, the persistence of NHBE cells is significantly greater when the cells move on LM332 than on fibronectin. Nonetheless, both BEP2D and NHBE cells display a higher rate of migration on LM332-coated substrates than on fibronectin. In addition, BEP2D cells move faster on the matrix of iHEK than on their own matrix, despite the former containing less LM332 than the latter. Because BEP2D matrix contains fibronectin, whereas iHEK cell matrix contains little, if any fibronectin, these results suggested to us that fibronectin might impede LM332-driven motility. We tested this possibility with our data indicating that the rate of migration of BEP2D and NHBE cells is reduced when the cells are plated onto iHEK matrix and/or LM332-coated surfaces supplemented with fibronectin, or when BEP2D cells move from their own matrix onto LM332/fibronectin–coated surfaces. At first glance, this may appear contrary to other studies showing that fibronectin promotes cell migration (6, 9, 11). However, it is consistent with our recent studies on skin cells, which also suggest that fibronectin impedes LM332-driven motility (18). Moreover, our adhesion data indicate that fibronectin enhances the "stickiness" of an LM332-rich matrix. This suggests that fibronectin likely slows migration by promoting firmer cell attachment to their substrate.

As part of these studies, we also investigated which laminin-binding integrin modulates the effect of LM332 on BEP2D cell motility. In previous studies on skin cells, we determined that knockdown of $\alpha6\beta4$ integrin down-regulates expression of $\alpha3\beta1$ integrin via effects on the phosphorylation state of 4EBP1 (20). Dephosphorylation of 4EBP1 disrupts its binding to eIF4E, allowing eIF4E to activate cap-dependent translation (26). We also knocked down $\alpha6$ integrin expression in BEP2D cells. This results in decreased $\beta4$ integrin expression. However, unlike iHEK, there is no commensurate dephosphorylation of 4EBP1 in $\alpha6$ integrin knockdown BEP2D cells (20). Thus, translation of the $\alpha3$ integrin subunit is maintained in such cells. This allowed us to evaluate migration of $\alpha6$ integrin knockdown BEP2D cells in the absence and presence of an $\alpha3$ integrin–blocking antibody. Our results demonstrate that $\alpha3\beta1$ integrin regulates the rate of migration of the cells moving on an LM332-rich matrix.

Whereas $\alpha6$ integrin knockdown human keratinocytes exhibit aberrant motility and fail to migrate directionally, $\alpha6$ integrin knockdown BEP2D cells move normally (20). Previously, we suggested that the explanation for the irregular motility behavior of $\alpha6$ integrin knockdown keratinocytes lies in their inability to deposit LM332 in trails onto the surface over which the keratinocytes move (20). Indeed, we have provided evidence in a number of studies that, in skin cells, "proper" LM332 deposition is $\alpha6\beta4$ integrin dependent (13, 28). The current results would appear to conflict with this. However, BEP2D (and NHBE) cells deposit fibronectin, in addition to LM332, onto their substrates. Moreover, fibronectin fibers outline the trails of LM332 in the matrix of both cell types. This raises the possibility that the organization of fibronectin in the matrix may determine the directed migration of moving cells, regardless of LM332 deposition. To test this possibility, we treated $\alpha6$ integrin knockdown BEP2D cells with fibronectin siRNA. Remarkably, the fibronectin-deficient and $\alpha6$ integrin knockdown BEP2D cells failed to show directed migration. These results are consistent with the notion that fibronectin, via its interaction with its integrin receptor, compensates for any misorganized LM332 with regard to supporting directed migration, in addition to its role in tempering cell speed when it is included in an LM332-rich matrix.

In summary, our results indicate that LM332, via $\alpha3\beta1$ integrin, determines the speed of migration of lung epithelial cells. Moreover, our results also provide new insights into the function of fibronectin in lung cell motility. We demonstrate that

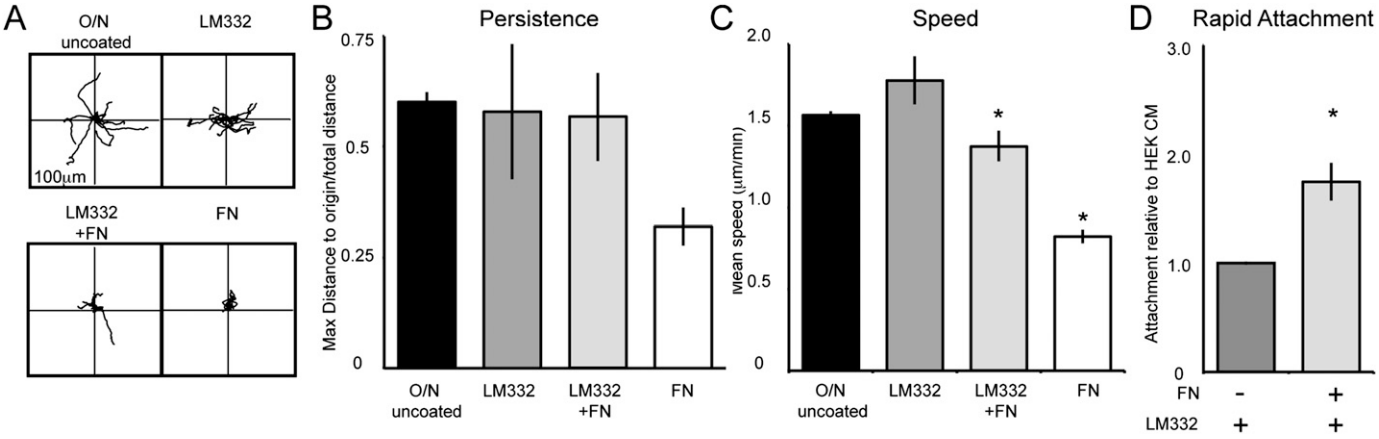

Figure 6. NHBE cell migration speed is regulated by FN in the matrix. (*A*) Vector diagrams depicting the individual migration patterns of ten randomly selected NHBE cells plated on an uncoated surface, LM332, LM332 supplemented with FN (LM332 + FN), or FN alone. The cells were allowed to adhere to the matrix for 2 hours and the migration of the cells was tracked for 1 hour. (*B* and *C*) Graphical representation of the persistence and speed of BEP2D cells as in (*A*). (*D*) A rapid attachment assay evaluating the adhesion of NHBE cells to LM332 or LM332 supplemented with FN (± FN) at 1 hour after plating. The individual *bars* of the graph represent mean (± SEM). All assays were performed in triplicate. For motility assays, roughly 60 cells were tracked per assay. *Significant differences, relative to cells migrating on or adhering to LM332, as determined by ANOVA and Student's *t* test.

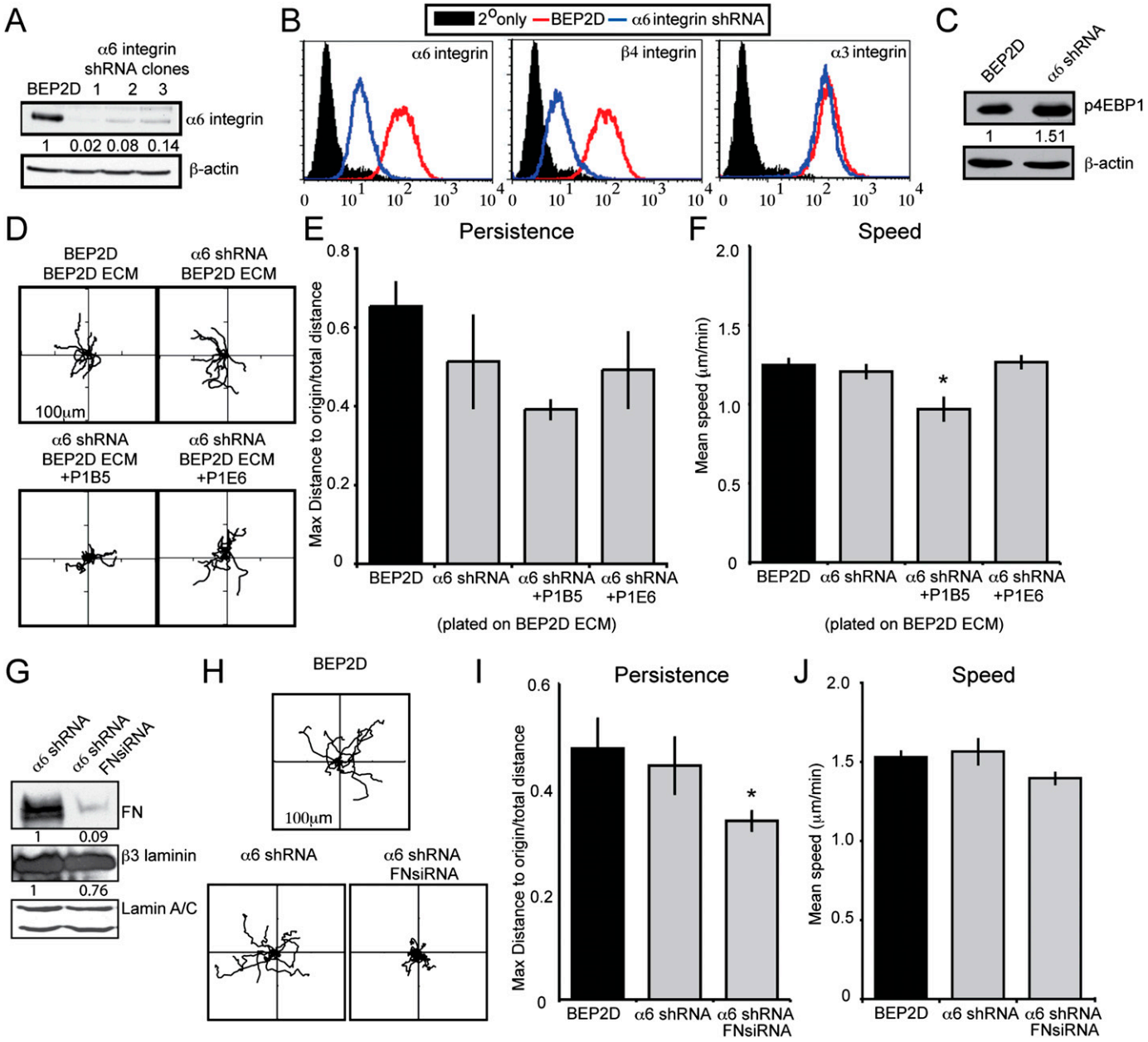

Figure 7. α3 integrin and α6 integrin roles in supporting BEP2D cell migration. (*A*) Immunoblotting analyses of wild-type (WT) BEP2D and three clones of BEP2D cells expressing lentivirus encoding α6 integrin small hairpin RNA (shRNA) using an α6 integrin antibody. Clone 3 was used in subsequent studies. (*B*) Surface expression of α6, β4, and α3 integrin subunits was measured in WT BEP2D cells (*red curves*) and clone 3 BEP2D cells exhibiting α6 integrin knockdown. *Filled curves* represent secondary antibody alone. (*C*) Extracts of BEP2D cells or clone 3 α6 integrin shRNA–expressing BEP2D cells were probed for levels of phosphorylated 4EBP1. β-actin was used as a loading control. (*D*) Rose plots of motility behavior of 10 randomly selected BEP2D and clone 3 α6 integrin shRNA–expressing BEP2D cells moving on BEP2D matrix in the presence or absence of inhibitory antibodies against α3 integrin (PIB5) or α2 integrin (P1E6). The cells were allowed to adhere to the matrix for 2 hours and the migration of the cells was subsequently tracked for 1 hour. (*E* and *F*) Graphical representation of persistence and speed of the cells as in (*D*). (*G*) Immunoblotting of clone 3 α6 integrin shRNA-expressing BEP2D and clone 3 BEP2D cells treated with FN siRNA (FNsiRNA). The same extracts were processed for immunoblotting with antibodies against β3 laminin and lamin A/C. In subsequent motility assays, unlike those shown in the previous figures, the motility of BEP2D cells was followed after overnight plating onto an uncoated substrate. (*H*) Rose plots of the motility behavior of 10 randomly selected α6 integrin shRNA–expressing BEP2D and clone 3 BEP2D cells treated with FN siRNA. (*I* and *J*) Graphical representation of persistence and speed of the cells as in (*H*). *Significance, $P <$ 0.05, relative to the migration of untreated clone 3 α6 shRNA BEP2D cells. Assays were performed in triplicate with roughly 60 cells tracked per assay.

fibronectin fine tunes the effects of other matrix molecules or complexes on lung cell migration. Indeed, fibronectin reduces the rate of cellular migration when lung cells move on an LM332-rich matrix by apparently enhancing cell–substrate adhesion. We speculate that, by doing so *in vivo*, fibronectin prevents the detachment of lung cells moving over a wound surface in the pulmonary environment where they are subject to considerable shear and stretch forces.

Author disclosures are available with the text of this article at www.atsjournals.org.

Acknowledgments: The authors are grateful for the gifts of cells and reagents from Drs. Curtis Harris (National Institutes of Health) and Caroline Damsky (University of California, San Francisco).

References

1. Djukanovic R. Airway inflammation in asthma and its consequences: implications for treatment in children and adults. *J Allergy Clin Immunol* 2002;109:S539–S548.
2. Puchelle E, Zahm JM, Tournier JM, Coraux C. Airway epithelial repair, regeneration, and remodeling after injury in chronic obstructive pulmonary disease. *Proc Am Thorac Soc* 2006;3:726–733.
3. Sacco O, Silvestri M, Sabatini F, Sale R, Defilippi AC, Rossi GA. Epithelial cells and fibroblasts: structural repair and remodelling in the airways. *Paediatr Respir Rev* 2004;5(Suppl A):S35–S40.
4. Coraux C, Roux J, Jolly T, Birembaut P. Epithelial cell–extracellular matrix interactions and stem cells in airway epithelial regeneration. *Proc Am Thorac Soc* 2008;5:689–694.
5. Amin K, Janson C, Sevéus L, Miyazaki K, Virtanen I, Venge P. Uncoordinated production of laminin-5 chains in airways epithelium of allergic asthmatics. *Respir Res* 2005;6:110.
6. Shoji S, Ertl RF, Linder J, Romberger DJ, Rennard SI. Bronchial epithelial cells produce chemotactic activity for bronchial epithelial cells: possible role for fibronectin in airway repair. *Am Rev Respir Dis* 1990;141:218–225.
7. McGowan SE. Extracellular matrix and the regulation of lung development and repair. *FASEB J* 1992;6:2895–2904.
8. White SR, Dorscheid DR, Rabe KF, Wojcik KR, Hamann KJ. Role of very late adhesion integrins in mediating repair of human airway epithelial cell monolayers after mechanical injury. *Am J Respir Cell Mol Biol* 1999;20:787–796.
9. Hérard AL, Pierrot D, Hinnrasky J, Kaplan H, Sheppard D, Puchelle E, Zahm JM. Fibronectin and its alpha 5 beta 1-integrin receptor are involved in the wound-repair process of airway epithelium. *Am J Physiol* 1996;271:L726–L733.
10. Legrand C, Gilles C, Zahm J-M, Polette M, Buisson A-C, Kaplan H, Birembaut P, Tournier J-M. Airway epithelial cell migration dynamics: MMP-9 role in cell–extracellular matrix remodeling. *J Cell Biol* 1999; 146:517–529.
11. Rickard KA, Taylor J, Rennard SI, Spurzem JR. Migration of bovine bronchial epithelial cells to extracellular matrix components. *Am J Respir Cell Mol Biol* 1993;8:63–68.
12. Willey JC, Broussoud A, Sleemi A, Bennett WP, Cerutti P, Harris CC. Immortalization of normal human bronchial epithelial cells by human papillomaviruses 16 or 18. *Cancer Res* 1991;51:5370–5377.
13. Sehgal BU, DeBiase PJ, Matzno S, Chew T-L, Claiborne JN, Hopkinson SB, Russell A, Marinkovich MP, Jones JCR. Integrin β4 regulates migratory behavior of keratinocytes by determining laminin-332 organization. *J Biol Chem* 2006;281:35487–35498.
14. Langhofer M, Hopkinson SB, Jones JC. The matrix secreted by 804G cells contains laminin-related components that participate in hemidesmosome assembly *in vitro*. *J Cell Sci* 1993;105:753–764.
15. Kligys K, Claiborne JN, DeBiase PJ, Hopkinson SB, Wu Y, Mizuno K, Jones JC. The slingshot family of phosphatases mediates Rac1 regulation of cofilin phosphorylation, laminin-332 organization, and motility behavior of keratinocytes. *J Biol Chem* 2007;282:32520–32528.
16. Tsuruta D, Hopkinson SB, Lane KD, Werner ME, Cryns VL, Jones JC. Crucial role of the specificity-determining loop of the integrin beta4 subunit in the binding of cells to laminin-5 and outside-in signal transduction. *J Biol Chem* 2003;278:38707–38714.
17. Gilles C, Polette M, Coraux C, Tournier JM, Meneguzzi G, Munaut C, Volders L, Rousselle P, Birembaut P, Foidart JM. Contribution of MT1-MMP and of human laminin-5 gamma2 chain degradation to mammary epithelial cell migration. *J Cell Sci* 2001;114:2967–2976.
18. Hamill KJ, Hopkinson SB, Hoover P, Todorović V, Green KJ, Jones JC. Fibronectin expression determines skin cell motile behavior. *J Invest Dermatol* 2012;132:448–457.
19. Mette SA, Pilewski J, Buck CA, Albelda SM. Distribution of integrin cell adhesion receptors on normal bronchial epithelial cells and lung cancer cells *in vitro* and *in vivo*. *Am J Respir Cell Mol Biol* 1993;8: 562–572.
20. Kligys KR, Wu Y, Hopkinson SB, Kaur S, Platanias LC, Jones JC. α6β4 integrin, a master regulator of expression of integrins in human keratinocytes. *J Biol Chem* 2012;287:17975–17984.
21. Goldfinger LE, Hopkinson SB, deHart GW, Collawn S, Couchman JR, Jones JC. The alpha3 laminin subunit, alpha6beta4 and alpha3beta1 integrin coordinately regulate wound healing in cultured epithelial cells and in the skin. *J Cell Sci* 1999;112:2615–2629.
22. Nguyen BP, Gil SG, Carter WG. Deposition of laminin 5 by keratinocytes regulates integrin adhesion and signaling. *J Biol Chem* 2000;275:31896–31907.
23. Ryan MC, Tizard R, VanDevanter DR, Carter WG. Cloning of the LamA3 gene encoding the alpha 3 chain of the adhesive ligand epiligrin: expression in wound repair. *J Biol Chem* 1994;269:22779–22787.
24. Choma DP, Milano V, Pumiglia KM, Dipersio CM. Integrin alpha3beta1-dependent activation of fak/src regulates rac1-mediated keratinocyte polarization on laminin-5. *J Invest Dermatol* 2007;127:31–40.
25. Frank DE, Carter WG. Laminin 5 deposition regulates keratinocyte polarization and persistent migration. *J Cell Sci* 2004;117:1351–1363.
26. McKendrick L, Pain VM, Morley SJ. Translation initiation factor 4E. *Int J Biochem Cell Biol* 1999;31:31–35.
27. Gingras AC, Raught B, Gygi SP, Niedzwiecka A, Miron M, Burley SK, Polakiewicz RD, Wyslouch-Cieszynska A, Aebersold R, Sonenberg N. Hierarchical phosphorylation of the translation inhibitor 4E-BP1. *Genes Dev* 2001;15:2852–2864.
28. Hamill KJ, Hopkinson SB, DeBiase P, Jones JC. BPAG1e maintains keratinocyte polarity through beta4 integrin–mediated modulation of Rac1 and cofilin activities. *Mol Biol Cell* 2009;20:2954–2962.